Multiferroic properties and exchange bias in $Bi_{1-x}Sr_xFeO_3$ ($x = 0$–0.6) ceramics*

Ma Zheng-Zheng(马争争)[a], Li Jian-Qing(李建青)[a], Chen Zi-Peng(陈子鹏)[a], Tian Zhao-Ming(田召明)[b], Hu Xiao-Jun(胡晓军)[a], and Huang Hai-Jun(黄海军)[a]†

[a] *Wuhan University of Technology, Wuhan* 430070, *China*
[b] *Huazhong University of Science and Technology, Wuhan 430074, China*

(Received 17 January 2014; revised manuscript received 28 March 2014; published online 23 July 2014)

Multiferroic properties and exchange bias (EB) in $Bi_{1-x}Sr_xFeO_3$ ($x = 0$–0.6) ceramics synthesized by a modified Pechini method are investigated. Sr concentration dependence of structure distorting, ferroelectric properties, and dielectric properties were studied at room temperature. Appropriate Sr doping ($x = 0.05$–0.2) has been found to decrease the conductivity, enhance ferroelectric properties and give rise to high dielectric constant. Compared with antiferromagnetic $BiFeO_3$ compound, BSFO-x ($0 \leq x \leq 0.4$) ceramics show weak ferromagnetism at room temperature, and their exchange bias field and vertical magnetization shift are observed and exhibit a strong dependence on the content of Sr. This observed EB effect which keeps stable in BSFO ceramics at 10 K tend to vanish at room temperature with Sr concentration over 0.4.

Keywords: multiferroic properties, ferroelectric properties, magnetic exchange bias, ferromagnetic properties

PACS: 75.80.+q, 75.85.+t, 77.84.–s **DOI:** 10.1088/1674-1056/23/9/097505

1. Introduction

Compounds which display coexistence of ferromagnetic (FM) and ferroelectric (FE) orders are known as multiferroic materials. Multiferroics have become an objects of growing interest due to the existence of magnetoelectric (ME) effect, which allows the reversal of the ferroelectric polarization by a magnetic field or the control of the magnetic order parameter by an electric field.[1–3] Unfortunately, the coexistence of ferromagnetism and ferroelectricity is difficult to achieve because the symmetry of the crystal structures prevents electric polarization. As a result, single-phase multiferroic materials rarely exist.[4]

Recently, $BiFeO_3$ (BFO)-based ceramics have been extensively studied.[5–9] BFO ceramic with a rhombohedrally distorted perovskite structure is an interesting candidate for its high FE Curie temperature (1083 K) and high Neel temperature ($T_N = 643$ K). However, a good polarization hysteresis (P–E) loop and a large remnant polarization in BFO is difficult to obtain, especially in the BFO ceramics, due to the high leakage current and low resistance caused by defects such as secondary phases and oxygen vacancies. The magnetic ordering of BFO has a spatially modulated spin structure which does not allow net magnetization and inhibits the observation of the linear magnetoelectric effect.

Extensive studies were carried out on rare-earth (RE) substitution in the A sublattice of the ABO_3 structure, such as La, Nd, Gd, etc.[10–16] The reason for choosing Sr is based on the interesting observations of approved ferromagnetic properties in BFO with A site substitution of Sr.[17–23] Ionic radius of Sr^{2+} is 1.18 Å, which is comparable to that of Bi^{3+} ion (1.03 Å). Bhushan *et al.* reported[19] a transformation from nearly rhombohedral to soherical geometry for 1–7 doping percentage of Sr in BFO nanoparticles. Our group[20] has reported the spin-glasslike behavior and exchange bias in 2/3 doping percentage of Sr in BFO ceramics at 10 K.

In this paper, $Bi_{1-x}Sr_xFeO_3$ ($x = 0$–0.6) ceramics (denoted as BSFO-x) have been successfully prepared by modified Pechini method. The structural, ferroelectric, dielectric, and magnetic properties of BSFO-x are presented. Appropriate Sr doping ($x = 0.05$–0.2) has been found to decrease the conductivity, enhance ferroelectric properties and give rise to high dielectric constant. In addition, magnetic measurement at room temperature showed that the exchange bias effect which changes with different Sr concentration in BSFO ceramics.

2. Experimental procedure

$Bi_{1-x}Sr_xFeO_3$ ceramics were synthesized by a modified Pechini method. First, bismuth nitrate pentahydrate $Bi(NO_3)_35H_2O$, iron nitrate enneahydrate $Fe(NO_3)_39H_2O$, and $Sr(NO_3)_2$ $4H_2O$ were dissolved into citric acid solution in stoichiometric proportions, with 5% excess bismuth nitrate to compensate bismuth loss during sintering process. The molar ratio of citric acid and the sum of metal ions (Sr^{2+}, Bi^{3+}, and Fe^{3+}) is 1:1–1.25:1. The solution was adjusted to a pH value of 7–8 by adding ammonia, and the mixture was dried at 150 °C to form gels. After that, the obtained gels were burned

*Project supported by the Program for New Century Excellent Talents in Universities of China (Grant No. 41322028), the Fundamental Research Funds for the Central University of China (Grant No. WUT 2014-Ia-018), and the National Science Fund for Excellent Young Scholars of China (Grant No. 41074056).

†Corresponding author. E-mail: hjhuang@whut.edu.cn

© 2014 Chinese Physical Society and IOP Publishing Ltd

and the precursory powder was calcined at 500 °C for 5 h. Finally, the powder was ground in an agate bowl for about 2 h, pressed into disks. The disks were sintered at 900 °C for 2 h, and subsequently quenched to room temperature to minimize the bismuth evaporation. Electrodes with silver coating were applied to both surfaces to measure the electrical properties.

The crystalline structure of the samples was examined by X-ray diffraction (XRD) (PANalytical B.V., X'Pert PRO, Holland). The magnetic properties were investigated by a commercial physical properties measurement system (Quantum Design, ppms-9, America). Polarization versus electric field (P–E) loops at room temperature was measured using a commercial FE test system (Premier II, Radiant Technologies). The dielectric properties of the ceramics were obtained with a precision impedance analyzer (6500B, WK, UK), with an AC voltage of 500 mA.

3. Results and discussion

Figure 1 displays the XRD patterns of the nominal series $Bi_{1-x}Sr_xFeO_3$ ceramics ($x = 0$–0.6). As can be seen in Fig. 1(a), there are several twin peaks in the XRD pattern of BFO viz [104] and [110], [006] and [202], [116] and [112], [018] and [214]. From Figs. 1(b) and 1(c), the relative intensity of these twin peaks changes with different x, and finally the twin peaks merge together to form a single peak, which indicates the distortion in the rhombohedral structure of BFO with signature of structural transformation. This is consistent with previous reports of bismuth-strontium ferrites.[24,25] Compared with the rhombohedral structure of BFO with space group R3c, all of the observed diffraction peaks from the BSFO samples with $x = 0.4$ and $x = 0.6$ is refined in the cubic space group $Pm3m$. The patterns of the samples with x between 0.05 and 0.2 indicate the coexistence of perovskite morphotrop21ic phase. Increasing the concentration of Sr causes all the peaks position to shift towards lower angles. This reveals a continual extension in lattice constant and also indicates that unit cell extended with the substitution of Sr^{2+} ion, which has a larger radius than Bi^{3+} ion.

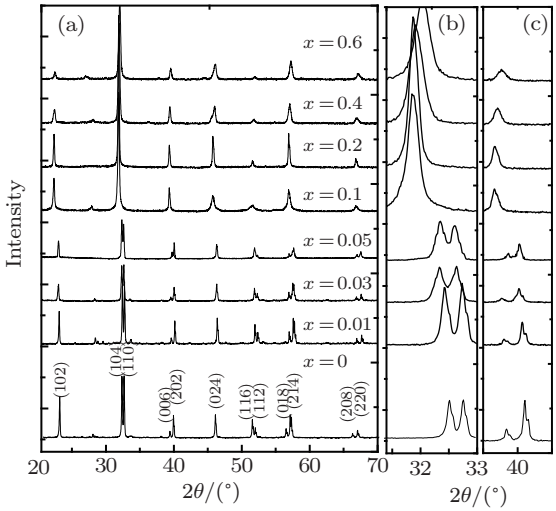


Fig. 1. The XRD patterns of $Bi_{1-x}Sr_xFeO_3$ ($x = 0$–0.6) ceramics compared with pure BFO ceramics.

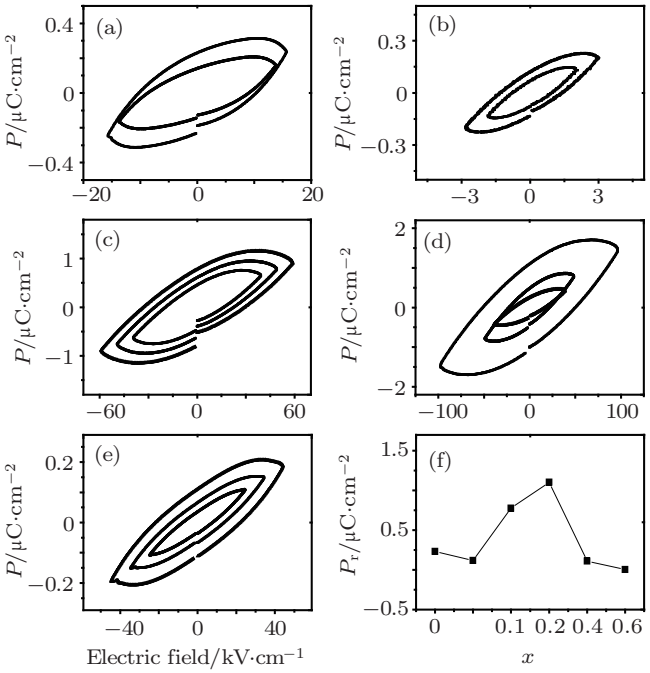


Fig. 2. Polarization hysteresis loops of $Bi_{1-x}Sr_xFeO_3$ ($x = 0$–0.4) ceramics at room temperature: (a) $x = 0$, (b) $x = 0.05$, (c) $x = 0.1$, (d) $x = 0.2$, and (e) $x = 0.4$. (f) Evolutions of P_r with the solubility x.

The ferroelectric behavior for BSFO samples is presented in Fig. 2. The $BiFeO_3$ exhibits an unsaturated hysteresis loop which is rounded at the highest field. Though $BiFeO_3$ is ferroelectric, the observed hysteresis loop is due to a large leakage current which can overshadow the real contribution from reorientation of electrical dipoles.[26] Although all the samples do not show saturated hysteresis loops, which is similar to the previous studies on BFO solid solution systems, the ferroelectric properties in our samples with Sr concentrations $0.05 \leq x \leq 0.4$ are much improved in comparison with that of $BiFeO_3$. Obvious ferroelectric behavior with large remnant polarizations (P_r) of 0.78 μC/cm^2 in BSFO-0.1 and 1.13 μC/cm^2 in BSFO-0.2 is observed. For the ferroelectric $x = 0.1$, $x = 0.2$ samples, the maximum polarization (P_m) and electric field (E_m) are 1.1508 μC/cm^2 at 32.85 kV/cm, and 1.73 μC/cm^2 at 67.97 kV/cm. This can be explained by the distortion of oxygen octahedral by a relative displacement of the equatoria and apical oxygens in Sr-doped samples as observed in A site ionsubstituted BFO,[27,28] The enhanced ferroelectricity suggests that the stereochemical activity of Bi lone electron pair plays an important role in the transition from ferroelectric to paraelectric state at $0.05 \leq x \leq 0.2$, which is similar to the previous studies on Bi-site ion doping BFO systems l.[29] As the content of Sr increases over 0.2, the P_r decrease

significantly with increasing x. This is evidence for the structure transformation to cubic.

In addition, dielectric properties of $Bi_{1-x}Sr_xFeO_3$ ($0.01 \leq x \leq 0.6$) have be investigated at room temperature. Figures 3 and 4 exhibit the variation of relative dielectric constant (ε_r) and loss tangent ($\tan\delta$) of BSFO-x with frequency. For all compositions, the dielectric constant decreases with increasing frequency, and remains fairly constant at higher frequency. All the curves all follow a dipole relaxation where at low frequencies the dipoles follow the frequency of the applied field. This is a normal behavior of ferroelectrics or dielectrics, which could be understood in terms of space charge relaxation.[30–32] The relationship of the frequency and tan δ for all samples reveals the presence of dielectric relaxation peaks, and the magnitude of the peaks deceases when x increases. For $x \geq 0.2$ samples, no obvious loss tangent peaks are observed.

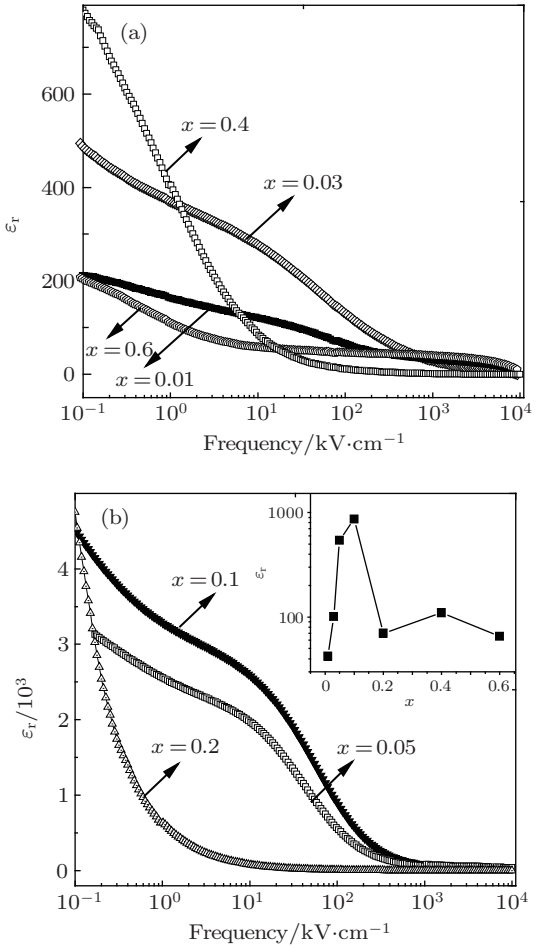


Fig. 3. Dielectric constant ε_r of $Bi_{1-x}Sr_xFeO_3$ ceramics at room temperature as a function of frequency. (a) $x = 0.01$, 0.03, 0.4, 0.6; (b) $x = 0.05$, 0.1, 0.2. Inset shows the variation in the value of ε_r measured at 100 kHz with the solubility x.

The dependence of dielectric constant and loss tangent at $f = 100$ kHz, with respect to Sr concentration in BFO, are shown in the inset of Figs. 3 and 4. There is a sharp rise in the ε_r value up to $x = 0.1$, followed the fall in the ε_r value as more Sr is doped. Our samples is much increased from 75 for pure BFO[33] to 891.12 for Sr = 0.1 at 1 kHz. The value of tan δ in our sample is kept between 1 and 2 when $x \leq 0.1$, but increases to 5–10 when the content of Sr is over 0.2. These improvements of ferroelectric and dielectric properties in BSFO ceramics can be ascribed to the appropriate substitution of Sr for Bi, which reduces the oxygen vacancies in the ceramics, resulting in a decrease in the contribution of the space charge polarization. For low Sr content, the dielectric constant of the samples increases and the dielectric loss of the samples decreases with increasing Sr content. This behavior can be qualitatively explained by interfacial polarization. The space charges tend to accumulate around the interfaces under an applied electric field and form an interfacial layer with a high relative dielectric constant and a low dielectric loss, resulting in an increase in the relative dielectric constant and a decrease in the dielectric loss. For high Sr content, the dielectric constant with a tetragonal structure decreases with decreasing c/a ratio and structure transition to cubic. This is similar to that of Ba-doped $BiFeO_3$ reported before.[34]

Field dependences of magnetization for the $Bi_{1-x}Sr_xFeO_3$ samples are shown in Fig. 5. The dependencies obtained for the $x = 0.01$ and $x = 0.03$ compounds practically coincide with the linear MH dependence in BFO, and

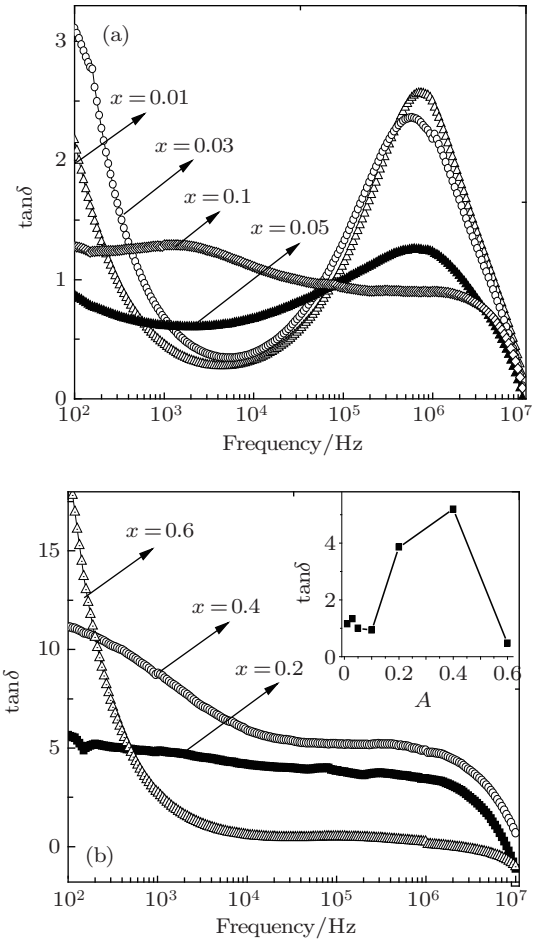


Fig. 4. Dielectric loss of $Bi_{1-x}Sr_xFeO_3$ ceramics at room temperature as a function of frequency. (a) $x = 0.05$, 0.01, 0.03, 0.1; (b) $x = 0.2$, 0.4, 0.6. Inset shows the variation in the value of tan δ measured at 100 kHz with the solubility x.

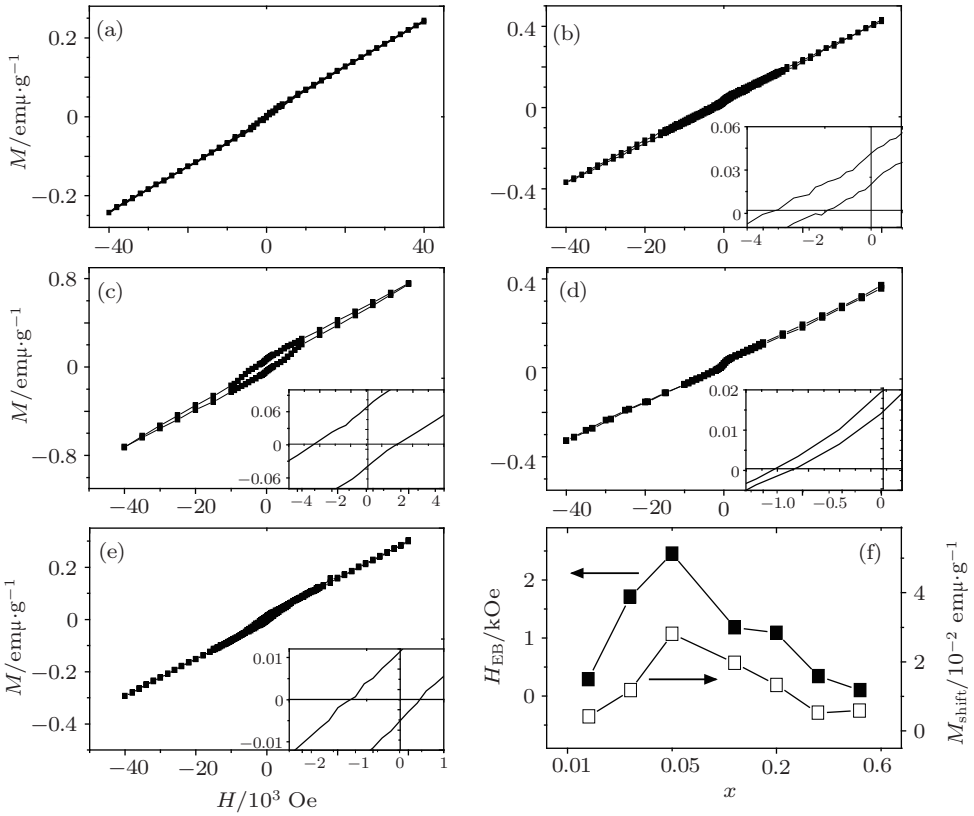


Fig. 5. Magnetization hysteresis loops of $Bi_{1-x}Sr_xFeO_3$ ceramics at room temperature: (a) $x = 0$, (b) 0.05, (c) $x = 0.1$, (d) $x = 0.2$, and (e) $x = 0.4$. (f) Evolutions of H_{EB} and M_{shift} with the solubility x.

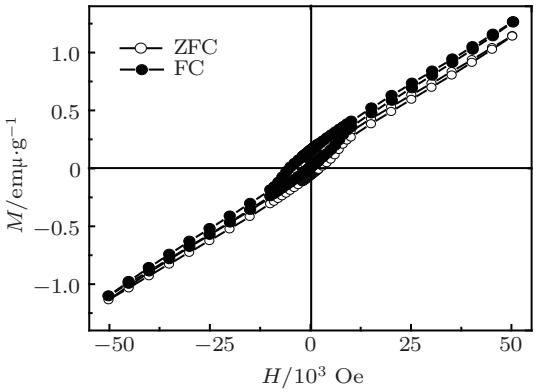


Fig. 6. Hysteresis loops of $Bi_{0.9}Sr_{0.1}FeO_3$ ceramics measured at 10 K after ZFC and FC. process in 50 kOe.

the net magnetization becomes apparent only at $x \geq 0.05$. The optimal FM behavior with remnant magnetization (M_r) of 0.067 emμ/g and coercive field (H_c) of 3.132 kOe is observed in $x = 0.1$ ceramics. M_r decreases as the content of Sr increases to 0.2, and reduces to zero when $x > 0.4$. A typical shift obtained for each sample is shown in the inset of Fig. 5. This shift of the hysteresis loops towards negative magnetic field axis was seen in all samples that support Neel's model of magnetization,[35,36] and indicates the presence of an exchange coupling between the antiferromagnetic core and the ferromagnetic.[20] The x dependence on exchange bias field (H_{EB}) and magnetization shift (M_{shift}) are plotted in Fig. 5(f). Both H_{EB} and M_{shift} increase as the content of Sr increases, and reach an maximum when $x = 0.05$. For $x > 0.1$ samples, the value of H_{EB} decreases as the concentration of Sr increases in the BSFO ceramics.

To further study the EB effect, the hysteresis loops for $x = 0.1$ sample have been measured at 10 K after zero-field-cooled (ZFC) and field-cooled (FC) process. As shown in Fig. 6, the ZFC hysteresis loop keeps a good central symmetry, while the FC hysteresis loop shows a negative exchange bias field which is much larger than what is observed at room temperature. It can be seen that H_{EB} decreased with increasing temperature for $x = 0.1$ sample. However, the EB effect is still present for $0.01 \leq x \leq 0.4$, which is quite different with the previous reports.[12,16] In Sr-doped BFO nanocrystalline samples reported before, the EB effect can only be observed in 10 K and vanish with temperature increased to room temperature. This appearance of M_{shift} is linked to the exchange coupling between FM clusters and the spin-glasslike (SGL) phases. During field cooling procedure, some of uncompensated spins of SGL phases are pinned along the cooling field direction and cannot be rotated with the field, which leads to the appearance of M_{shift}. It also can be found that the FC hysteresis loop displace an increased magnetization compared with ZFC counterparts. This may be contributed from the uncompensated spins of SGL phases where the FC process increases the number of the spins rotatable with the FM clusters.

4. Conclusion

The structural, magnetic, and ferroelectric properties of the phase pure $Bi_{1-x}Sr_xFeO_3$ ceramics ($x = 0$–0.6) prepared by a modified Pechini method are investigated. Appropriate Sr doping ($x = 0.05$–0.2) has been found to decrease the conductivity, enhance ferroelectric properties and give rise to high dielectric constant. In addition, magnetic measurement at room temperature showed that the exchange bias effect which changes with different Sr concentration in BSFO ceramics.

References

[1] Sang W C and Maxim M 2007 *Nat. Mater.* **6** 13
[2] Spaldin N A and Fiebig M 2005 *Science* **309** 391
[3] Eerenstein W, Mathur N D and Scott J F 2006 *Nature* **442** 759
[4] Wang J, Neaton J B, Zheng H, Nagarajan V, Ogale S B, Liu B, Vinhjand D, Vaithyanathan V, Schlom D G, Waghmare U V, Spaldin N A, Rabe K M, Wuttig M and Ramesh R 2003 *Science* **299** 1719
[5] Jia D C, Xu J H, H Ke, Wang W and Zhou Y 2009 *J. Eur. Ceram. Soc.* **29** 3099
[6] Ivanov S A, Nordblad P, Tellgren R and Ritter C 2010 *Solid State Science* **12** 115
[7] Gu Y H, Liu Y, Yao C, Ma Y W, Wang Y, Chan H L W and Chen W P 2014 *Chin. Phys. B* **23** 037501
[8] Ma Z Z, Li J Q, Tian Z M, Qu Y and Yuan S L 2012 *Chin. Phys. B* **21** 107503
[9] Song Z W and Liu B G 2013 *Chin. Phys. B* **22** 047506
[10] Yuan G L and Siu W O 2006 *Appl. Phys. Lett.* **88** 062905
[11] Jyoti R S and Rao C N R 2007 *Solid State Sciences* **9** 950
[12] Zhang X q, Sui Y, Wang X J, Wang Y and Wang Z 2010 *J. Alloy. Compd.* **507** 157
[13] Das R and Mandal K 2012 *J. Magn. Magn. Mater.* **324** 1913
[14] Varshney D, Sharma P, Satapathy S and Gupta P K 2014 *J. Alloy. Compd.* **584** 232
[15] Li J B, Rao G H, Xiao Y G, Luo J, Liu G Y, Chen J R and Liang J K 2010 *Chin. Phys. B* **19** 107505
[16] Lin P T, Li X, Zhang L, Yin J H, Cheng X W, Wang Z H, Wu Y C and Wu G H 2014 *Chin. Phys. B* **23** 047701
[17] Folcke E, Breton J M L, Bréard Y and Maignan A 2010 *Solid State Science* **12** 1387
[18] Moure A, Tartaj J and Moure C 2011 *J. Alloy. Compd.* **509** 7042
[19] Bhushan B, Basumallick A, Vasanthacharya N Y, Kumar S and Das D 2010 *Solid State Sciences* **12** 1063
[20] Tian Z M, Yuan S L, Zheng X F, Jia L C, Huo S X, Duan H N and Liu L 2010 *Appl. Phys. Lett.* **96** 142516
[21] Balamurugan K, Kumar N H and Santhosh P N 2009 *J. Appl. Phys.* **105** 07D909
[22] Kundys B, Maignan A, Martin C, Nguyen N and Simon C 2008 *Appl. Phys. Lett.* **92** 112905
[23] Yu X L and An X Q 2009 *Solid State Commun.* **149** 711
[24] Sati P C, Arora M, Chauhan S, Kumar M and Chhoker S 2014 *J. Phys. Chem. Sol.* **75** 105
[25] Singh V, Sharma S, Kumar M, Kotnala R K and Dwivedi R K 2014 *J. Magn. Magn. Mater.* **349** 264
[26] Levin I, Karimi S, Provenzano V and Dennis C L 2010 *Phys. Rev. B* **81** 020103
[27] Li J, Duan Y, He H and Song D 2001 *J. Alloys Compd.* **315** 259
[28] Khomchenko V A, Kiselev D A, Kopcewicz M, Maglione M and Shvartsman V 2009 *J. Magn. Magn. Mater.* **321** 1692
[29] Yang C, Liu C Z, Wang C M, Zhang W G and Jiang J S 2012 *J. Magn. Magn. Mater.* **324** 1483
[30] Yuan G L and Siu W O 2006 *Appl. Phys. Lett.* **89** 052905
[31] Pandit P, Satapathy S, Gupta P K and Sathe V G 2009 *J. Appl. Phys.* **106** 114105
[32] Dai Z H and Akishige Y K 2010 *J. Phys. D: Appl. Phys.* **43** 445403
[33] Jaiparkash, Kumar Y, Chauhan R S and Kumar R 2011 *Solid State Science* **13** 1869
[34] Yang C, Jiang J S, Qian F Z, Jiang D M, Wang C M and Zhang W G 2010 *J. Alloy. Compd.* **507** 29
[35] Ohldag H, Scholl A, Nolting F, Arenholz E, Maat S, Young A T, Carey M and Stöhr J 2003 *Phys. Rev. Lett.* **91** 017203
[36] Tian Z M, Yuan S L, Yin S Y, Liu L, He J H, Duan H N, Li P and Wang C H 2008 *Appl. Phys. Lett.* **93** 222505